CHAPTER V
PREPARATION AND CHARACTERIZATION OF MULTI-WALLED CARBON NANOTUBE FILLED THE BLEND OF PVDF/BC FILMS

5.1 Abstract

In this work, the effect of carboxyl multi-walled carbon nanotube (MWCNT) loading on bio-nanocomposite films of PVDF/BC blend (90/10) were investigated on piezoelectric and dielectric properties based on the basis of flexible piezoelectric touch sensor. The dielectric enhancement was found at 5 phr of MWCNT which a conductive phase (MWCNT) influenced to increase dielectric constant about 9 orders of magnitude at frequency of 10 MHz - 1 GHz and temperature of 80°C. The activation energy of dielectric relaxation in tertiary blend of PVDF/BC/MWCNT were calculated using the Arrhenius relationship at 293-373 K. The in-plane piezoelectric coefficient (d_{33}) and polarization-electric filed (P-E) hysteresis loop were enhanced as increasing the amount of MWCNT. Dynamic mechanical analysis indicated significant improvement in storage modulus in comparison with that of $PVDF_{90}BC_{10}$ films.

5.2 Introduction

A piezoelectric material have ability to create an electrical signal when subject to mechanical stimuli (direct piezoelectric effect). This basis of piezoelectricity can be used as force, touch, pressure and mechanical sensor (Tressler *et al.*, 1998). Recently, polymers have been recovery the piezoelectric characteristic due to their dipole orientation and polarization (Shuford, 1977). Piezoelectric polymers can overcome limitation of common piezoelectric ceramics: heavy, brittle and difficult to process.

However, the piezoelectric coefficient of polymer is much lower than ceramic materials. In order to realize piezoelectricity, the piezoelectric coefficient (d_{ij}) are related through the dielectric constant (ε_o) while applied mechanical stress which approximately equal to $d_{ij} = \varepsilon_o/g_{ij}$, where ε_o is the vacuum dielectric constant

permittivity ($8.85x10^{-12}$ F/m). However, the dielectric constant of polymer is relatively low ($\varepsilon \sim 3$). The enhancement in dielectric constant can be achieved by adding conductive phase with small amount based on percolation theory. The polymer/conductive composite possess lightweight and flexibility (He, 2009) compared to original polymer/ceramic composite.

The conductivity of multi-walled carbon nanotube (MWCNT) arise from the motion of electron along π-system, MWCNT also promises nano-scale filler, high aspect ratio, lightweight, and good electro-mechanical properties. The side-wall of MWCNT can be functionalized to improve the miscibility of composite. In this work, the carboxyl-MWCNT was introduced to PVDF/BC (90/10 by weight) blend. The carboxyl group of the nanotube created partially miscible with F atoms of PVDF and O atoms with bacterial cellulose.

The PVDF/BC/MWCNT composite films are mainly characterized the essential properties for piezoelectric touch sensor. The d_{33} coefficient and remanent polarization were highest at MWCNT 3 phr loading to composite. The tertiary blends composed of two crystalline phases (α and β). The 5 phr MWCNT loaded film exhibited higher storage modulus that other compositions and no absence of β' mechanical relaxation region.

5.3 Experimental Procedures

5.3.1 Materials

Nata de coco was purchased from local food factory as a food grade. PVDF (J100) was supplied by Asambly Chemicals Company. N,N-dimethylformamide (DMF) and sodium hydroxide (NaOH) were purchased from RCI Labscan Co.,Ltd. and Merck Ltd., respectively. Carboxylic treated multi-walled carbon nanotube (>95% of carbon nanotube content) was purchased from Chengdu Organic Chemicals Company, Chinese Academy of Sciences, People Republic of China. The average diameter and length are less than 10 nm and 30 μm as written in the technical data sheet.

5.3.2 Extraction and Purification of Bacterial Cellulose

Bacterial cellulose (BC) was extracted from nata de coco product. The nata de coco gel were firstly rinsed with distilled water and blended using a laboratory blender. Then, nata de coco gel was treated with 0.1 M NaOH at 80°C for 1 hour to remove any remaining microorganisms, medium component and soluble polysaccharides. The purified bacterial cellulose will be then thoroughly washed with distilled water until reached the neutral pH.

5.3.3 Fabrication of PVDF/BC-MWCNT Nanocomposite Films

The nanocomposite films were firstly prepared by solvent casting technique. DMF was used as solvent to dissolve PVDF at 60°C and stirred until the homogeneous solution was obtained. Then, BC and PVDF were mixed together at the desired weigh ratio 10/90. The MWCNT were dispersed in DMF using an ultrasonic probe for 30 minutes then filled in the mixture of BC/PVDF at different weight precent loading. The mixtures were stirred at 60°C for 30 minutes to allow good distribution then poured on Petri dish glass. After the solvent was vaporized in an oven at 80°C for 48 hours in order to remove all remaining solvent, the casted film of BC/PVDF were obtained. Then, hot-pressed technique was used to make a dense film. The casted nanocomposites were cut into pellets, heated at 180°C for 20 minutes, followed by 10 tons of pressure for 5 minutes. Finally, the films were about 0.5 mm in thickness.

5.3.4 Characterizations

The β phase of crystalline formation of PVDF in the blends were investigated using Fourier transform infrared spectroscopy (Nicolet, NEXUS 640) via ATR mode. The crystalline phase behavior of the blends also confirmed X-ray diffractometer (XRD). The dielectric constant and dissipation factor were measured using a Network Analyzer (Agilent, E4991A) at the frequency ranging from 10 MHz to 1 GHz and temperature of -50-100 °C. The thermal transitions of each compositions, T_g, T_m and T_d, were investigated by DSC. Dynamic mechanical analysis was performed in tension mode using a GABO, EPLEXOR 100N at a constant frequency of 1 Hz to studies dynamic mechanical properties at temperature

of -50-200 °C. The ferroelectric properties was performed using P-E hysteresis loop and d_{33}meter (APC Int. Ltd., model 8000) at room temperature.

5.4 Results and Discussion

5.4.1 Crystalline Phase Behavior

The $PVDF_{90}BC_{10}$ was studied the effect of MWCNT content (phr) on crystalline phase formation of the films. The β crystalline phase (all-trans planar zigzag conformation) of PVDF part has highest piezoelectricity and pyroelectricity. Thus, the amount of β phase is used to indicate the piezoelectric properties of materials. The FTIR spectra of $PVDF_{90}BC_{10}$ and $PVDF_{90}BC_{10}$-MWCNT blend films are shown in Figure 5.1, all of blend films consisted of two important phases refer to α (763 and 976 cm^{-1}) and β (510 and 840 cm^{-1}) phase.

The calculated β phase content, F(β), of the blends are summarized in Table 5.1. The F(β) of different MWCNT loading to $PVDF_{90}BC_{10}$ matrix were fluctuated from 45.71 -60.58 %. Due to the agglomeration of MWCNT disrupted the ability of crystalline formation, PVDF molecules in the blend try to form in the easiest conformation (α phase). The highest F(β) was observed in composite film of MWCNT 1phr as high as 60.58%.

Table 5.1 β-phase contents, F(β) (%), of $PVDF_{90}BC_{10}$ with various MWCNT (phr) loading

MWCNT (phr)	β-phase contents, F(β) (%)
0	63.25
1	60.58
2	45.71
3	54.19
4	48.31
5	56.76

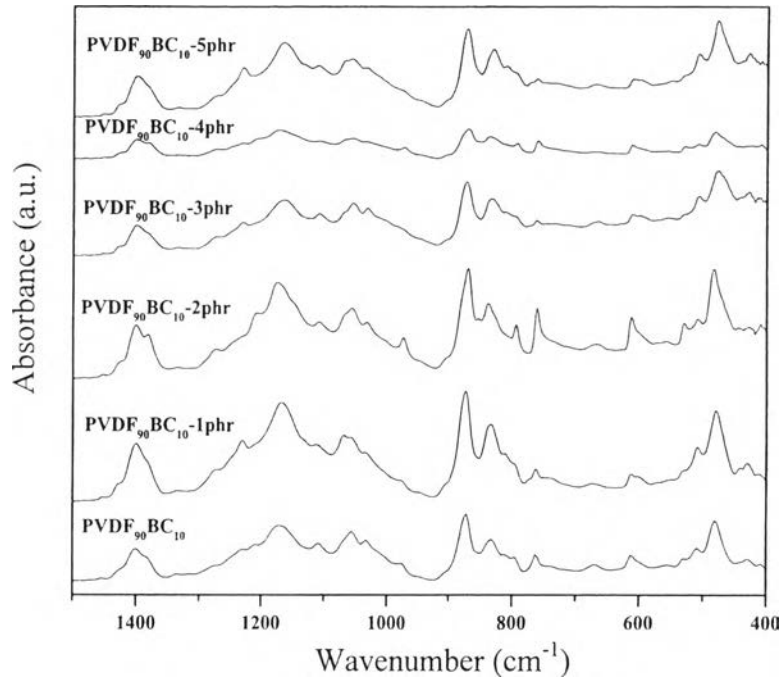

Figure 5.1 FTIR spectra of $PVDF_{90}BC_{10}$ and $PVDF_{90}BC_{10}$-MWCNT blend films.

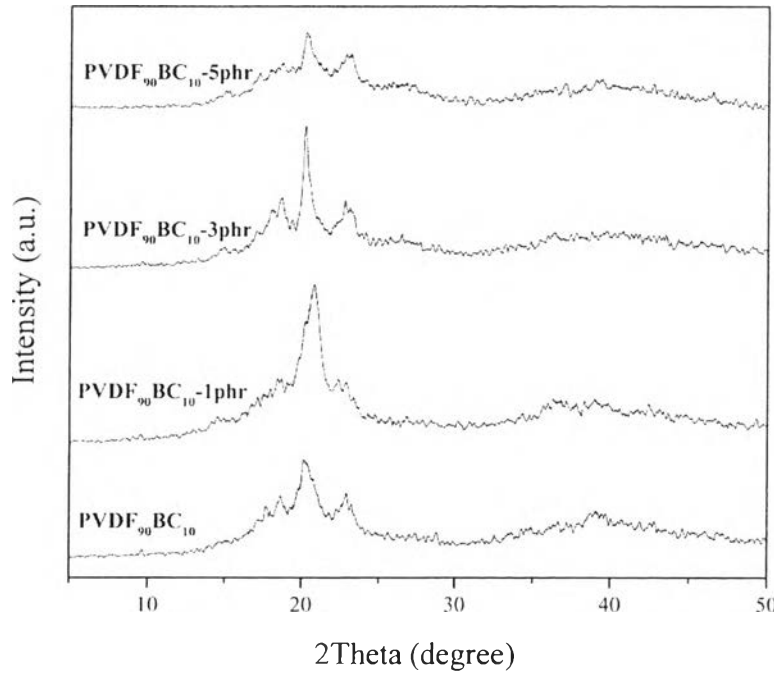

Figure 5.2 XRD diffractograms of $PVDF_{90}BC_{10}$ and $PVDF_{90}BC_{10}$-MWCNT blend films at 1, 3 and 5 phr.

XRD measurement was performed to identify the crystal phase behavior the composite films. The broad XRD peak implies the mixing of crystalline and amorphous region as shown in Figure 4.2. The β crystalline phase, orthorhombic structure, shows the diffraction peaks in 2θ Bragg angle at 20.4°, 36.7° and 40°. Nevertheless, the peak of α crystalline phase exhibited at 27° refer to (021) diffraction plane. The ratio of β/α phase of the blends was increased as increasing MWCNT content up to 3 phr. This XRD result can be concluded that the compressed films yielded both of β and α phases and the amount of MWCNT effect to the crystal formation of the films.

5.4.2 Thermal Transition Observation

The second heating DSC thermograms of all sample were characterized of consumes glass transition temperature (T_g) and melting temperature (T_m) as shown in the Figure 5.3 and their corresponding data are presented in the Table 5.2. The combination of MWCNT has effect to molecular motion in amorphous region of PVDF part. The T_g of tertiary blend of PVDF/BC/MWCNT films were increased from -40.02°C ($PVDF_{90}BC_{10}$) to as high as -36.39°C ($PVDF_{90}BC_{10}$-MWCNT 4 phr).

According to the basis of bacterial cellulose (BC), a natural polymer, has strong hydrogen bonding between its chain, which the unmodified BC has no T_m. The T_m of all of the blend films refer to PVDF matrix only. The T_m of tertiary blend were slightly lower than $PVDF_{90}BC_{10}$ (based composition of each tertiary blends). These T_m data were related to the β phase content of the films. Adding MWCNT resulted in lower F(β), the β phase has better chain packing than other phase of PVDF crystalline. Thus, higher F(β) will require higher temperature to melt the β crystalline phase. The % crystallinity, X_c, indicate the amount of crystalline region in the blend films. The result found that MWCNT did not much effect to X_c, which signified that MWCNT did not hindered the migration and diffusion of PVDF molecular chain to form crystalline region. Except MWCNT 4 phr loading, this composition can acts as nucleating agent which yield to higher % crystallinity, T_g and T_m than other compositions.

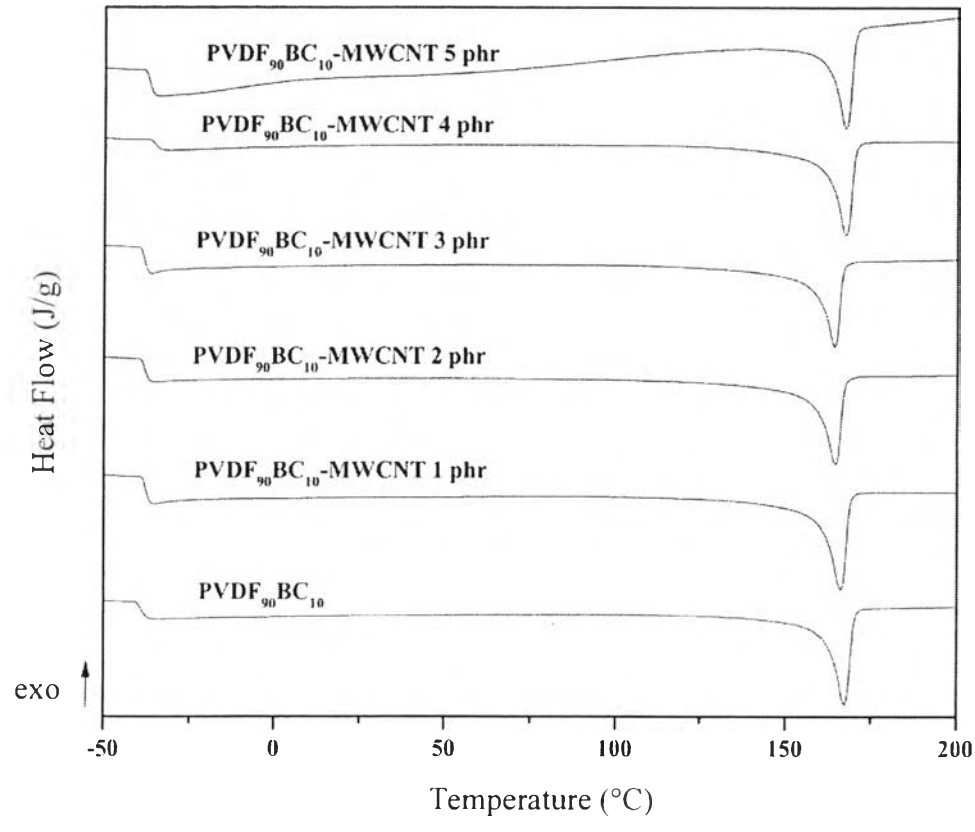

Figure 5.3 DSC second-heating curves of $PVDF_{90}BC_{10}$ at various MWCNT (phr) loading.

Table 5.2 DSC parameters of $PVDF_{90}BC_{10}$ at various MWCNT (phr) loading

MWCNT (phr)	ΔH_m(J/g)	T_g (°C)	T_m (°C)	X_c (%)
0	33.10	-40.02	162.01	35.8
1	32.72	-38.55	160.70	35.4
2	30.86	-38.90	159.18	33.4
3	31.59	-39.13	158.92	34.2
4	34.17	-36.39	162.00	37.0
5	32.86	-37.90	161.95	35.6

*Heat of fusion value for 100% crystalline PVDF, ΔH_0= 102.7 J/g

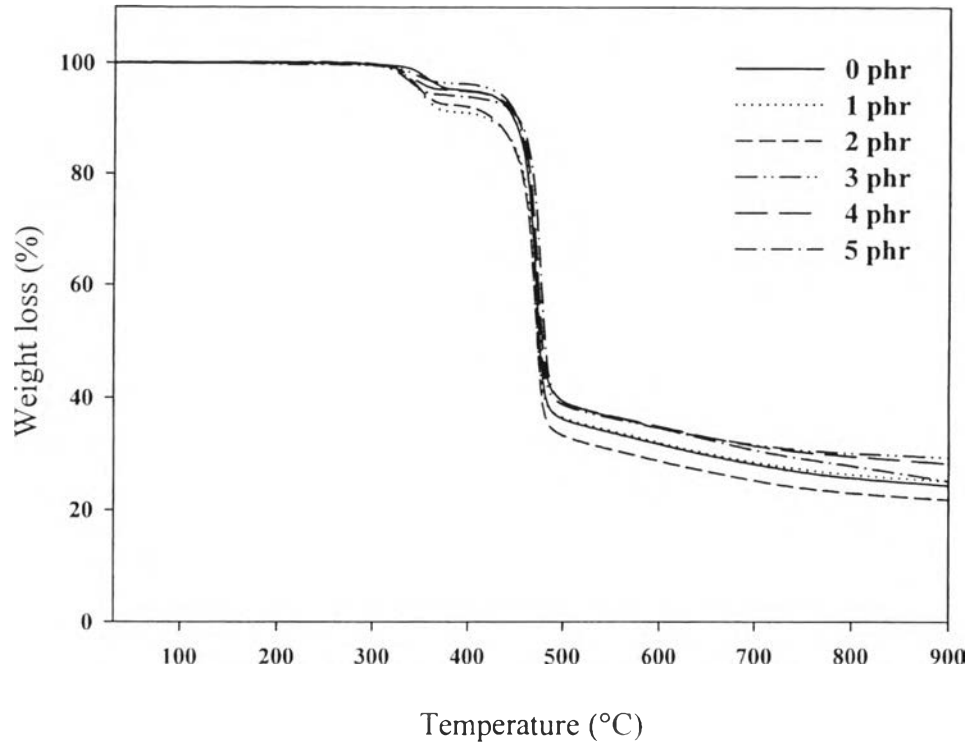

Figure 5.4 TG-DTA thermograms of $PVDF_{90}BC_{10}$ at various MWCNT (phr).

The introduction of BC in PVDF caused increasing in thermal stability because intermolecular interaction between polar atoms as described in Chapter IV. From TGA curves (Figure 5.4), $PVDF_{90}BC_{10}$ and $PVDF_{90}BC_{10}$-MWCNT blend films were found two steps of weight loss. The first degradation region refer to anhydroglucose ring of BC start to decompose at temperature around 320-340 °C. The second degradation step corresponding to PVDF part, the degradation temperature is similar about 470 °C, the result demonstrated that MWCNT has no effect to improve the thermal stability of PVDF polymeric chain. Moreover, it can be found that these blend systems were being free from DMF as solvent and any water absorption since no loss step of water and solvent was shown at temperature lower than 150 °C.

5.4.3 Dynamic Mechanical Properties

The relaxation of polymer blends were investigated by DMA technique to indicate the performance of material under an applied force and temperature. The thermal evaluations of compressed $PVDF_{90}BC_{10}$ were shown in Figure 5.5 and 5.6. The measurement were carried out over a range of temperature (-80°C to 150°C) at a constant frequency of 1Hz.

Figure 5.5 shows the storage moduli (E') of $PVDF_{90}BC_{10}$ and $PVDF_{90}BC_{10}$-MWCNT blend films. As observed, the storage modulus decreased non-linearly with increasing temperature. The addition of MWCNT also showed the improving in the storage modulus significantly. MWCNT 5 phr loading exhibited highest storage modulus while temperature above 50°C refer to no absence of β' relaxation in the films, MWCNT disrupted molecules in amorphous regions created fold part and had smaller change in loss modulus compared to other compositions.

The DMA dissipation factor curves (Figure 5.6), three relaxation regions were observed corresponding to β, β' and α relaxation, respectively. First relaxation was found at -40°C which is a dynamic glass transition temperature (T_g), called β relaxation resulting from molecular movement in amorphous region. The T_g of all compressed films shift to higher temperature due to pressure press cause molecule rearranged into better chain packing. Moreover, the sharp increase in dissipation factor of compressed films also observed at about 60°C corresponding to the β' relaxation. This weak relaxation raised from compressing force made molecules in amorphous region became folded. The third relaxation called α relaxation was associated with segmental motion in crystalline regions, exhibited at around 150°C which close to melting temperature of PVDF.

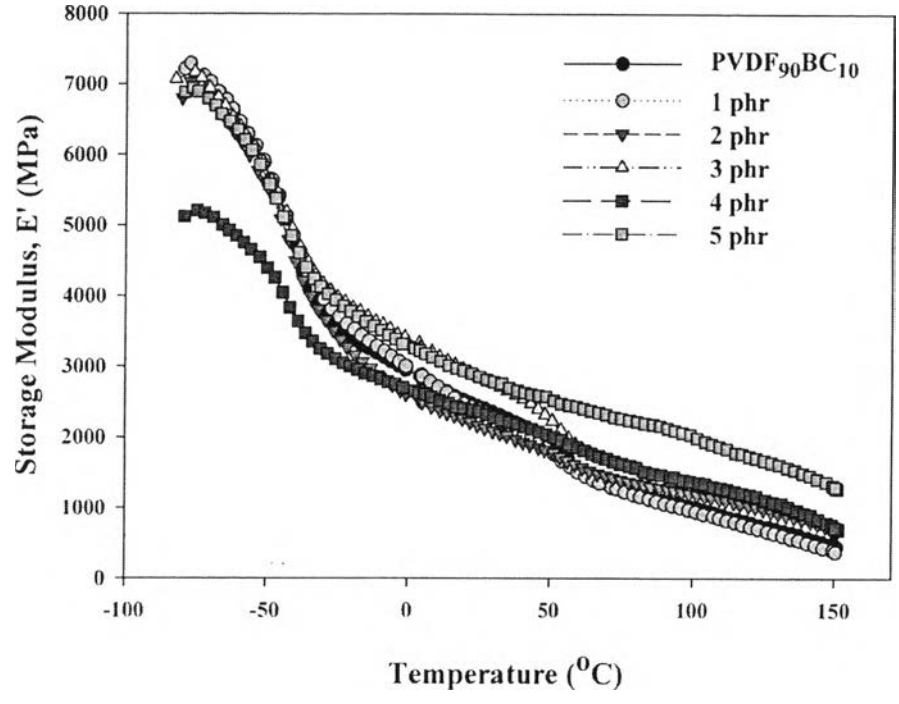

Figure 5.5 Storage tensile modulus, E' vs. temperature of $PVDF_{90}BC_{10}$ film with various MWCNT loading.

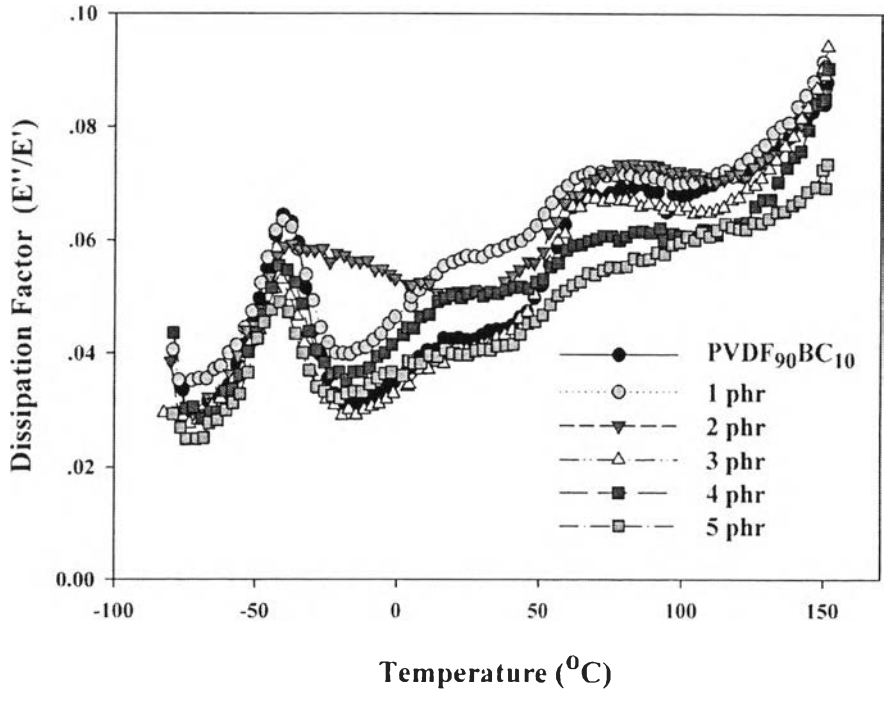

Figure 5.6 Dissipation factor (E''/E') vs. temperature of $PVDF_{90}BC_{10}$ film with various MWCNT loading.

5.4.4 Dielectric Behavior

5.4.4.1 The Effect of MWCNT on Dielectric Properties

As one of the most important conductive fillers, MWCNT possesses high dielectric permittivity at the amount of filler close to their percolation threshold, the point that conductive filler create conducting pathway.

The Figure 5.7 (a) and (b) show dielectric constant and dissipation factor as a function of temperature (20, 50 and 80 °C) and amount of conductive filler (MWCNT) loading to $PVDF_{90}BC_{10}$ matrix. As predicted by percolation threshold theory, the dielectric constant of composite of conducting phase (MWCNT) and insulating dielectric phase ($PVDF_{90}BC_{10}$) presented a large increase in dielectric constant, $\varepsilon' \sim 72$ at 80°C with frequency of 10MHz when the amount of MWCNT close to percolation threshold (5phr). MWCNT content also effect to the dissipation factor which was dramatically increased due to it started to create percolating MWCNT network. As compared the dielectric behavior of MWCNT composite to both of neat PVDF and $PVDF_{90}BC_{10}$ films (Figure 5.8 (a) and (b)),the results exhibited that the dielectric constant was improved about 9 times at temperature higher than 70°C when added MWCNT 5 phr.

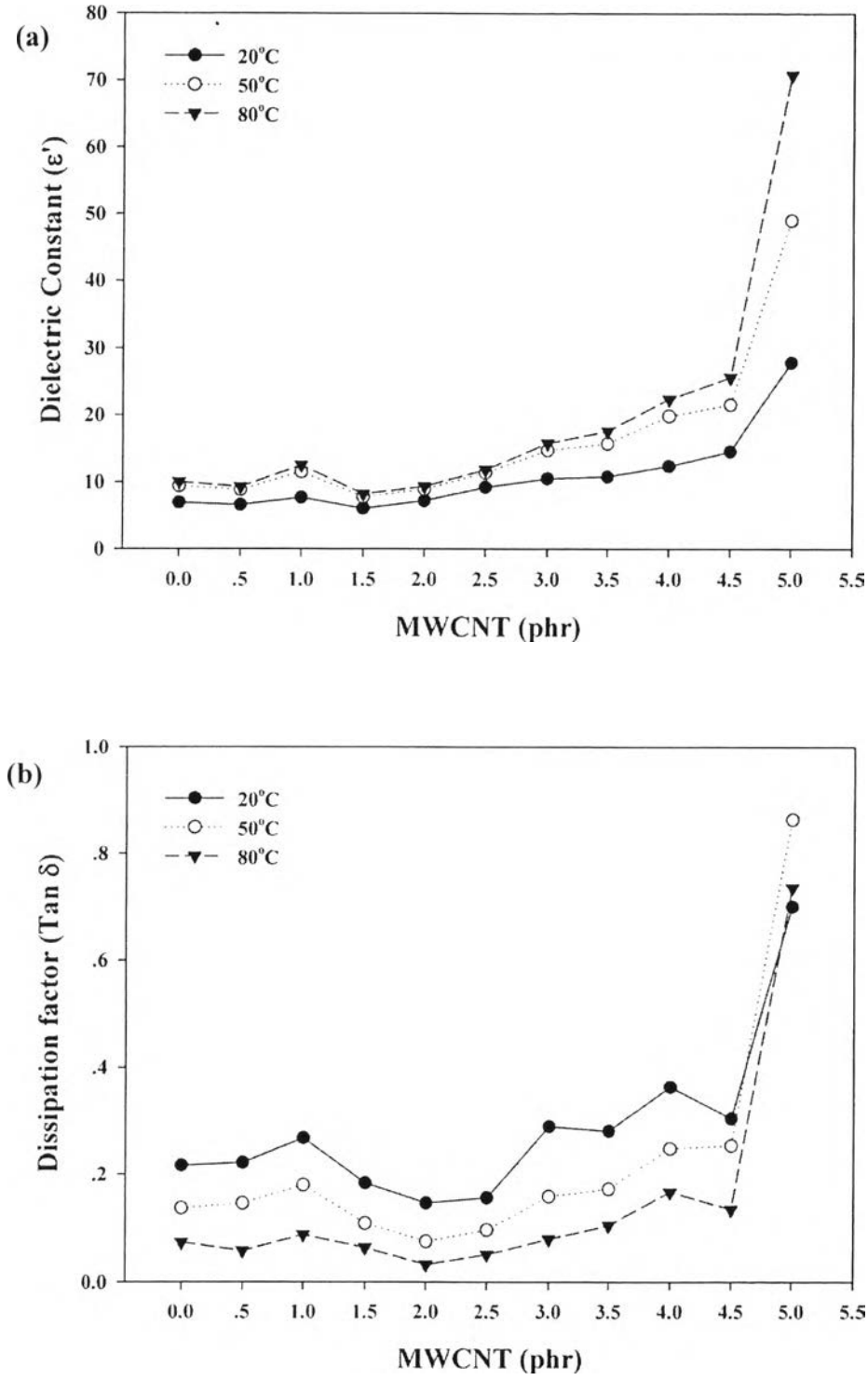

Figure 5.7 Dielectric constant (a) and dissipation factor (b) of various MWCNT (phr) loading to $PVDF_{90}BC_{10}$ matrix measured at 10MHz and temperature (20, 50 and 80°C).

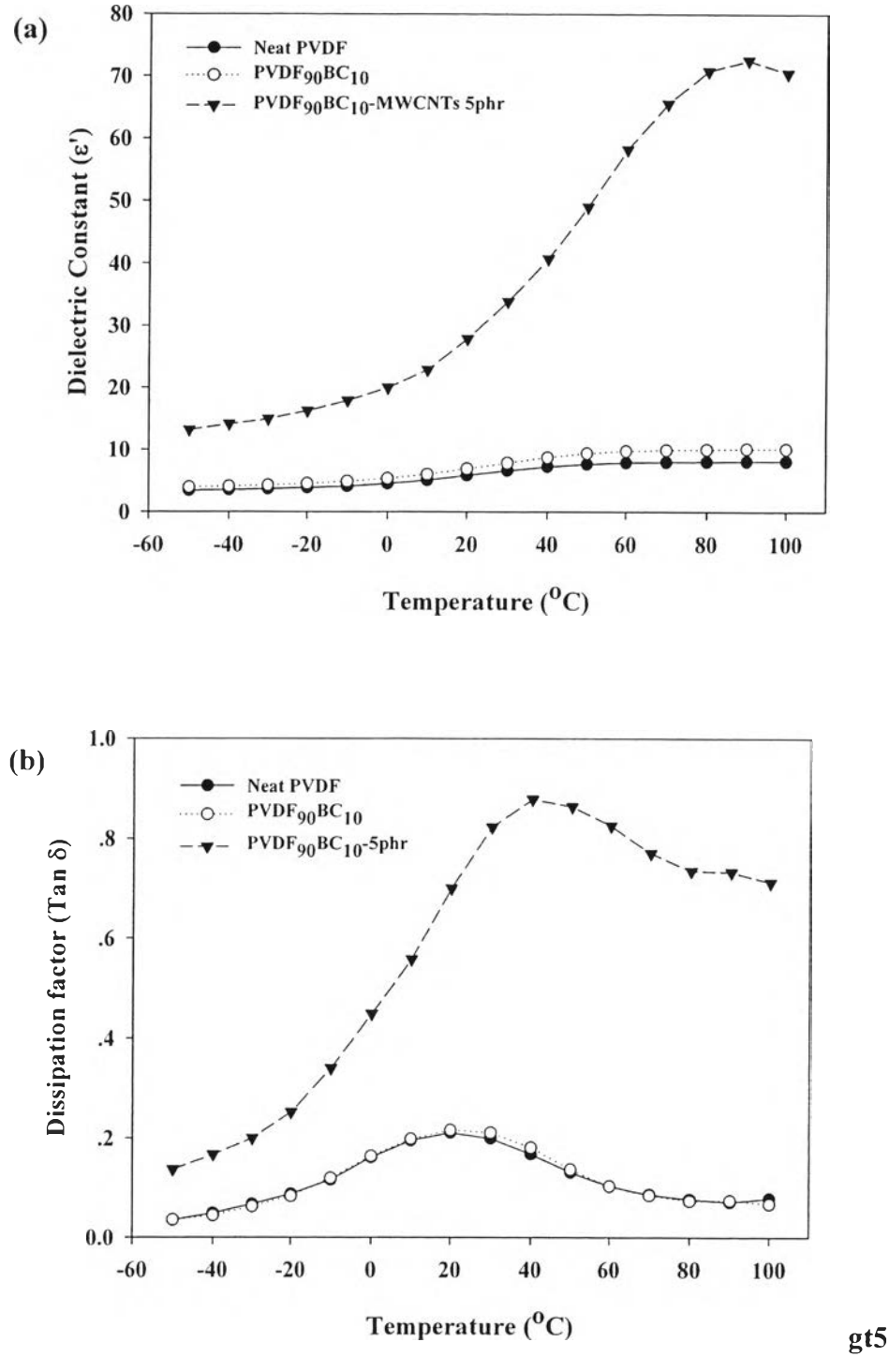

Figure 5.8 Dielectric constant (a) and dissipation factor (b) of neat PVDF, $PVDF_{90}BC_{10}$ and $PVDF_{90}BC_{10}$-MWCNT 5phr films as a function of temperature (°C) at 10 MHz.

5.4.4.2 Dielectric Relaxation Behavior

As observation from Figure 5.8b, the dissipation factor exhibited a single relaxation behavior as increasing temperature. These results demonstrated that the dielectric loss of composite film also showed single relaxation state at temperature range from 270 to 345 K as shown in Figure 5.9-5.10. This dielectric loss phenomena can be described using Arrhenius law (Hilczer, 2002; Chanmal, 2008; Rekik, 1023), which is valid for Debye-like loss mechanism as following equation:

$$\tau = \tau_0 \exp\left(\frac{E_a}{kT}\right)$$

Where k is the Boltzmann's constant (8.314×10^{-15} eV/K), T is the maximum relaxation temperature, τ_0 is the time constant.

$$\ln \tau = \ln \tau_0 + \left(\frac{E_a}{kT}\right)$$

The E_a can be calculated from the slope of ln τ vs. 1/T and τ_0 is an intersect with the vertical axis

For blend system, a single relaxation of dielectric constant corresponds to the miscibility of the blend (Rao, 2002). This result indicated that both of binary and tertiary blend in this research showed partially miscible due to the interaction between polar atoms. The temperature dependent of dielectric relaxation process is further analyzed by fitted with Arrhenius relationship to determine E_a and relaxation time as shown in Figure 5.11. The fitting parameters for dielectric relaxation are shown in Table 5.3. The relaxation peak associated with the molecular motions in PVDF crystalline region which arise from various imperfections like chain rotations within the interior of crystalline phase. The activation energy, E_a, of tertiary blend was increase when the amount of MWCNT up to 2 phr. In contrast, adding higher MWCNT contens yield to decreased E_a about 1 eV implied that the higher amorphous phases resulted in requiring lower E_a to activated the molecular chain.

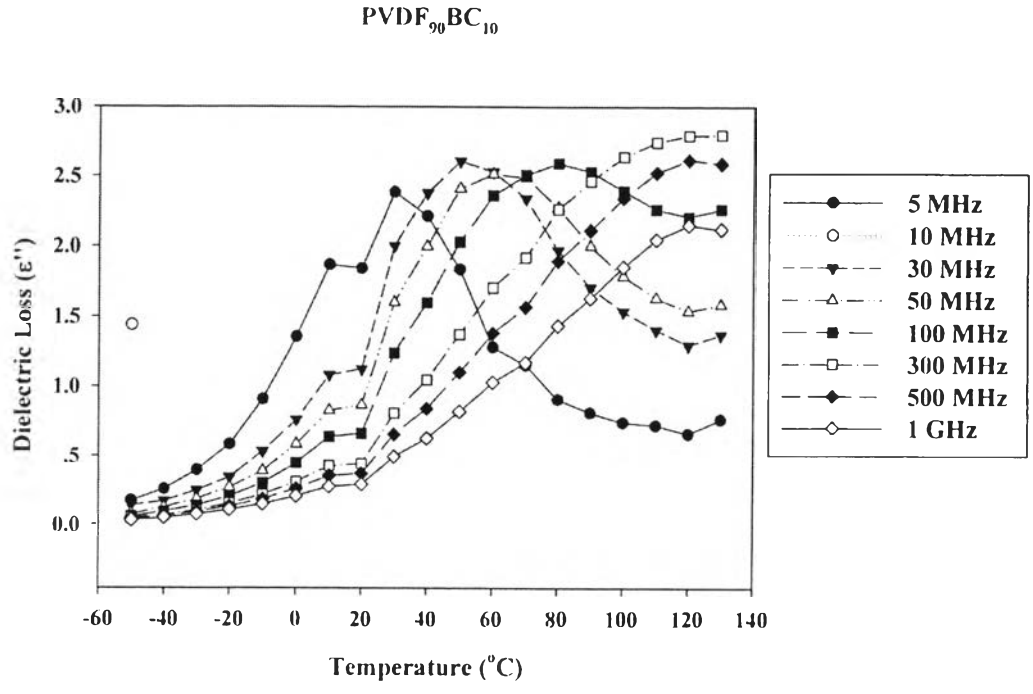

Figure 5.9 Dielectric loss (ε'') curves of $PVDF_{90}BC_{10}$ films at temperature -50°C - 130°C.

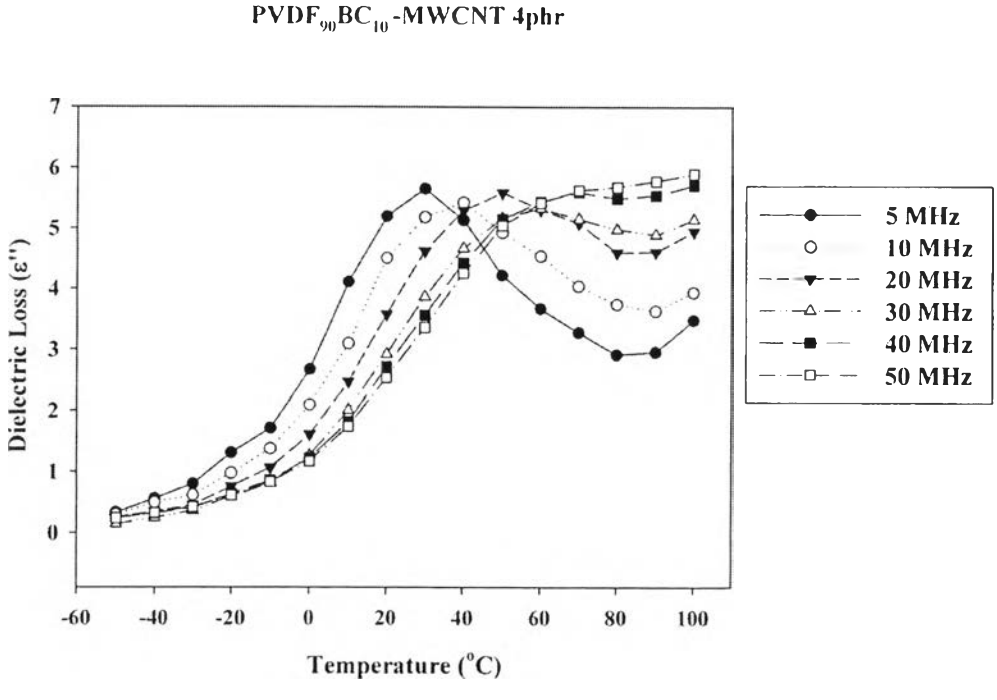

Figure 5.10 Dielectric loss (ε'') curves of $PVDF_{90}BC_{10}$-MWCNT 4 phr films at temperature -50°C - 100°C.

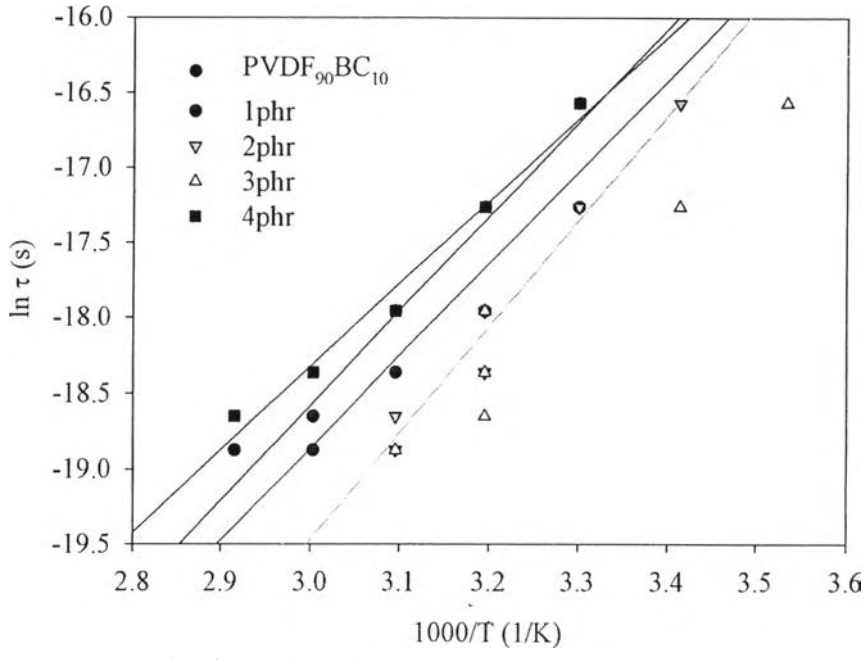

Figure 5.11 Arrhenius plot, logarithum of relaxation time versus reciprocal temperature of dielectric loss of $PVDF_{90}BC_{10}$ and $PVDF_{90}BC_{10}$-MWCNT blend films showing the Arrhenius relationship.

Table 5.3 The analysis of dielectric loss relaxation process by the Arrhenius relationship of $PVDF_{90}BC_{10}$ and $PVDF_{90}BC_{10}$-MWCNT blend films

MWCNT (phr)	τ_o (sec)	E_a (eV)
0	5.72×10^{-17}	0.522
1	6.91×10^{-17}	0.587
2	2.29×10^{-18}	0.586
3	7.79×10^{-16}	0.428
4	7.70×10^{-16}	0.457

5.4.5 Ferroelectric Properties

The non-centro symmetry of othorhombic structure (β-phase) of PVDF and moniclinic structure of cellulose can generate piezoelectricity. In this section, the polarization measurement were performed to understand the ferroelectric behavior of neat PVDF, $PVDF_{90}BC_{10}$ and $PVDF_{90}BC_{10}$-MWCNT blend films.

The polarization (P, $\mu C/cm^2$) of the nanocomposite films were investigated as a function of an applied electric field (E, kV/cm) to studied ferroelectric behavior at room temperature. The polarization-electric field (P-E) hysteresis loop of neat PVDF films were measured in the range of 80-140 kV/cm as shown in Figure 5.12. It shows weak ferroelectric properties with small remanent polarization (P_r, hysteresis intersect the vertical axis) and coercive field (E_c, hysteresis intersect the horizontal axis). The maximum polarization increase with increasing E but the spontaneous polarization is not occur at room temperature due to PVDF molecule need higher energy to switch the direction of vinyl chains.

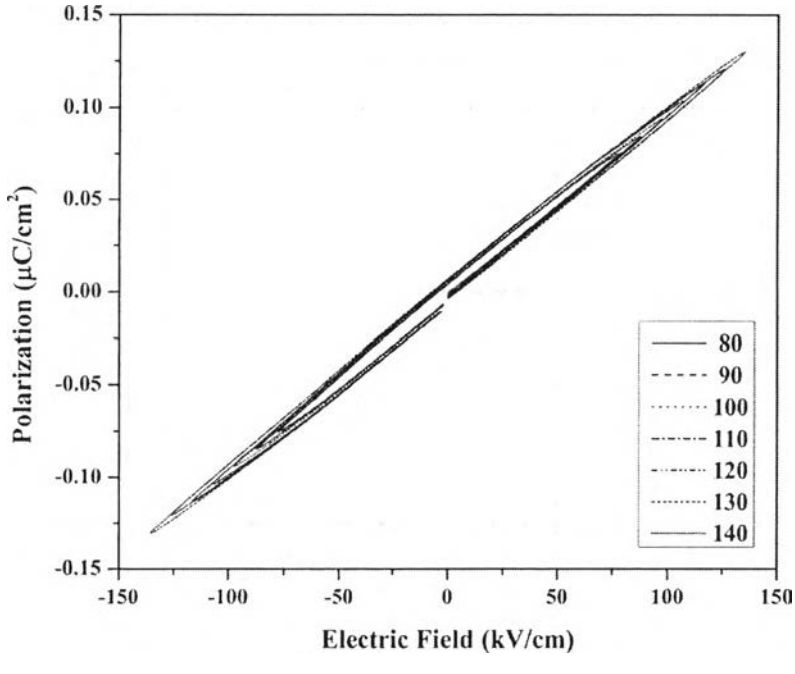

Figure 5.12 P-E hysteresis loop of neat PVDF films at room temperature.

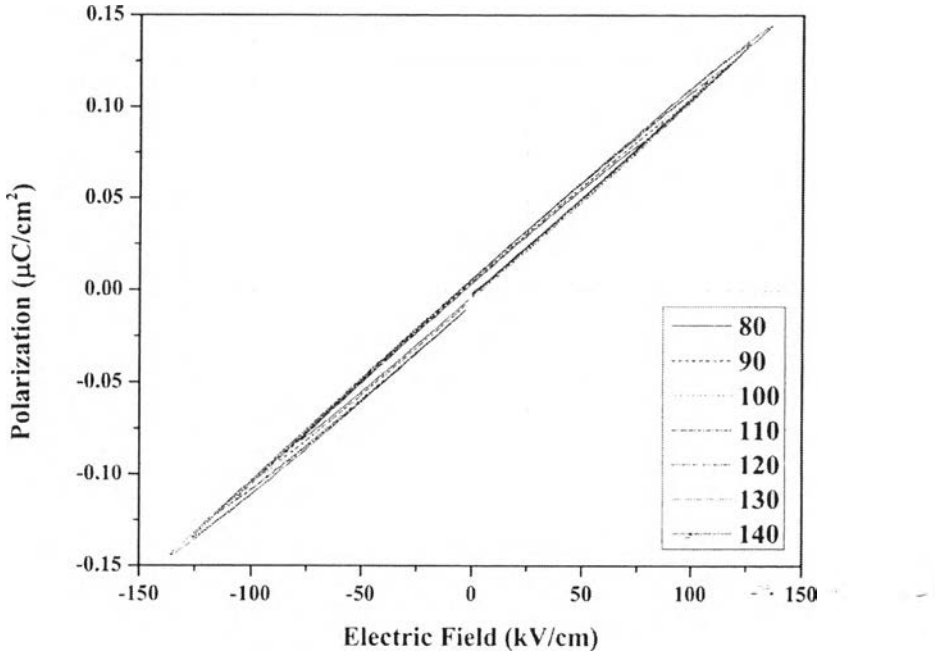

Figure 5.13 P-E hysteresis loop of $PVDF_{90}BC_{10}$ films at room temperature.

The polarization behavior of $PVDF_{90}BC_{10}$ films (Figure 5.13) was similar to neat PVDF which the P_r of those films was about 0.006 and -0.012 $\mu C/cm^2$. The results demonstrated that even the F(β) of $PVDF_{90}BC_{10}$ (63.25 %) was less than the neat one (71.42 %) but the polarization was anhanced from dipolar orientation of bacterial cellulose chain.

The effect of MWCNT contents (phr) loading to $PVDF_{90}BC_{10}$ film on P-E hysteresis loop were investigated as shown in Figure 5.14 and corresponding datas are shown in Table 5.4. The highest P_r was obtained from $PVDF_{90}BC_{10}$-MWCNT 3 phr film which higher than that of $PVDF_{90}BC_{10}$ about 5 times. The enhancement in P_r obtained from electron between graphene ring can polarize along the nanotube. However, with increasing the amount of MWCNT up to 5 phr, the polarization behavior was not enhanced as expected due to the aggregation of the nanotube. The poor dispersing of conductive filler cannot improve the polarization of composite film.

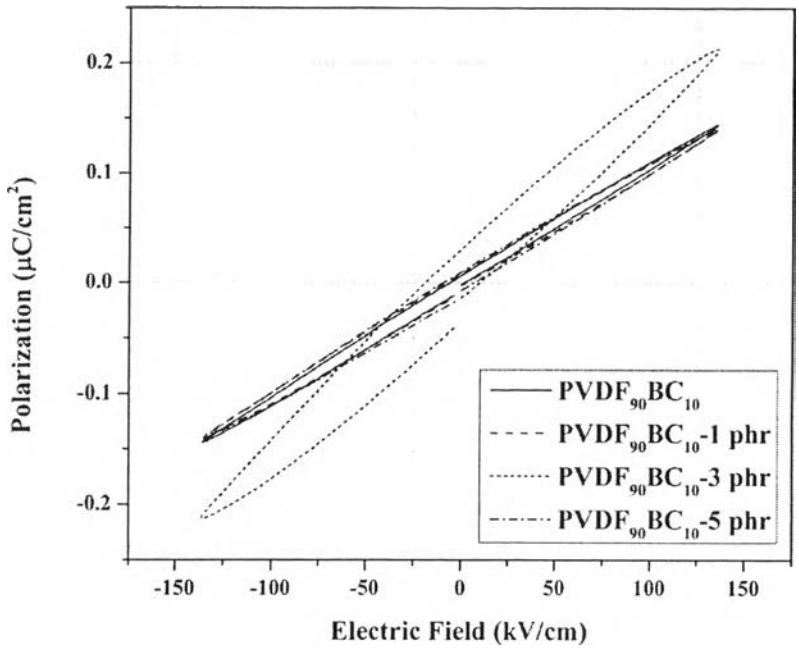

Figure 5.14 P-E hysteresis loop of $PVDF_{90}BC_{10}$ with various amount of MWCNT at room temperature.

Table 5.4 The polarization profile of $PVDF_{90}BC_{10}$ and $PVDF_{90}BC_{10}$-MWCNT blend films

MWCNT (phr)	P_{Max} ($\mu C/cm^2$)	P_r ($\mu C/cm^2$)	$-P_r$ ($\mu C/cm^2$)	V_c (kV/cm)	$-V_c$ (kV/cm)
0	0.1442	0.0063	-0.0121	37.755	-138.087
1	0.1400	0.0084	-0.0140	83.166	-208.968
3	0.2118	0.0306	-0.0415	208.447	-393.095
5	0.1406	0.0099	-0.0178	160.175	-214.492

5.4.6 Piezoelectric Properties

Before investigated the in-plane stress piezoelectric coefficient, all samples were subjected to corona charging process at a constant of electric field 40kV/cm, room temperature for 60 minutes, to obtain the charge separation inside of the films.

Piezoelectric behavior of the corona poled films was investigated using d_{33} meter to measured in-plane piezoelectric coefficient which the direction of applied stress and measured charged are the same. As FTIR spectra in Figure 4.5 and 5.1, PVDF composites were clearly form in β polymorph which its orthorhombic structure exhibit piezoelectric behavior. The unpoled samples showed d_{33} values (Table 5.5) about -(10-11) pC/N, after poling the d_{33} coefficient reached -15 pC/N with the addition of MWCNT 3 phr. Thus, it can be suggest that d_{33} coefficient increased with an increasing MWCNT and remanent polarization of the nanocomposite films.

Table 5.5 Piezoelectric coefficient, d_{33} (pC/N) of PVDF and its blends

Material	**Piezoelectric coefficient, d_{33} (pC/N)**	
	Before Poling	**After Poling**
PVDF	-10	-11
$PVDF_{90}BC_{10}$	-10	-11
$PVDF_{90}BC_{10}$- MWCNT 1phr	-11	-12
$PVDF_{90}BC_{10}$- MWCNT 3phr	-11	-15
$PVDF_{90}BC_{10}$- MWCNT 5phr	-10	-14

5.5 Conclusions

The carboxyl multi-walled carbon nanotube filled PVDF/BC (90/10) blends were prepared using solvent casting followed by compression technique. The crystalline phase behavior of the blend composed of two crystalline phases (α and β) as demonstrated by FTIR spectra and XRD patterns. The storage modulus was decrease non-linearly with increasing temperature and dynamic mechanical relaxation contributed to 3 regions (β, β' and α transitions) . The MWCNT 5 phr can improved dielectric constant about 9 times compared to neat PVDF and $PVDF_{90}BC_{10}$ films. A single dielectric loss was found in each composition indicated the partially miscible of this tertiary blend system. As increasing the amount of MWCNT to 3 phr, the P_r showed highest value as 0.0306 $\mu C/cm^2$ which 5 order of $PVDF_{90}BC_{10}$ matrix, the d_{33} coefficient reached -15 pC/N. On the basis of these results, this bio-composite films are promising to use as flexible piezoelectric touch sensor.

5.6 Acknowledgement

This work was completely investigated the piezoelectric and ferroelectric properties through helpful with Asst. Prof. Dr. Naratip Vittayakporn (King Mongkut's Institute of Technology Ladkrabang), Asst. Prof. Dr. Theerachai Bongkarn (Naresuan University) and Dr. Teerapon Yamwong (National Metal and Materials Technology Center). The authors would like to acknowledge the financial support from the National Research Council Thailand (NRCT), grant number GRB_BSS_66_56_63_08, and The Petroleum and Petrochemical College (PPC), Chulalongkorn University.

5.7 References

Chanmal, C.V.and Jog, J.P. (2008) Dielectric relaxations in PVDF/BaTiO3 nanocomposites. Polymer Letters, 2(4), 294–301.

He, F., Lau, S., Chan, H.L., and Fan, J. (2009) High Dielectric Permittivity and Low Percolation Threshold in Nanocomposites Based on Poly(vinylidene fluoride) and Exfoliated Graphite Nanoplates. Advanced. Materials, 21, 710–715.

Hilczer, B., Kułek, J., Markiewicz, Ewa., Kosec, M., and Mali, B. (2002) Dielectric relaxation in ferroelectric PZT–PVDF nanocomposites. Journal of Non-Crystalline Solids, 305, 167–173.

Rao,V., Ashokan, P.V., and Amar J.V. (2002) Studies on Dielectric Relaxation and Ac Conductivity of Cellulose Acetate Hydrogen Phthalate–Poly (vinyl pyrrolidone) Blend. Journal of Applied Polymer Science, 86, 1702–1708.

Rekik, H., Ghallabi, Z., Royaud, I., Arous, M., Seytre, G., Boiteux, G., and Kallel, A. (2013) Dielectric relaxation behaviour in semi-crystalline polyvinylidene fluoride (PVDF)/TiO2 nanocomposites. Composites: Part B, 45, 1199–1206.

Shuford, R.J., Wilde, A.F., Ricca, J.J., and Thomas, G.R. (1977) Piezoelectric Polymer Films for Application in Monitoring Devices. Army Materials and Mechanics Research Center. Watertown, Massachusetts.